CPXM1: a novel biomarker for gastric cancer prognosis

Jun Du
Department of Gastrointestinal Surgery, The First Affiliated Hospital of Wannan Medical College
Mengxiang Zhu
Department of Gastrointestinal Surgery, The First Affiliated Hospital of Wannan Medical College
Wenwu Yan
Department of Gastrointestinal Surgery, The First Affiliated Hospital of Wannan Medical College
Changsheng Yao
Department of Gastrointestinal Surgery, The First Affiliated Hospital of Wannan Medical College
Qingyi Li
Department of Gastrointestinal Surgery, The First Affiliated Hospital of Wannan Medical College
Jinguo Wang (shwangjg@sina.com)
Department of Gastrointestinal Surgery, The First Affiliated Hospital of Wannan Medical College

Research Article

Keywords: gastric cancer, CPXM1, immunohistochemistry, prognosis evaluation, bioinformatics analysis

Posted Date: March 22nd, 2021

DOI: https://doi.org/10.21203/rs.3.rs-337128/v1

Abstract

Background

The molecular role of carboxypeptidase X, M14 family member (CPXM1) in oncogenesis or tumor progression remains unclear. The aim of this study was to determine whether CPXM1 can be used as a potential prognostic biomarker for gastric cancer (GC).

Methods

We first demonstrated the relationship between CPXM1 expression and GC in various public databases. Secondly, the expression of CPXM1 in GC tissues was further verified by immunohistochemical staining using tissue microarray containing 96 cases of GC patients. Kaplan–Meier analysis and a Cox proportional hazard regression model were performed to evaluate the relationship between the expression of CPXM1 and the survival of GC patients. Finally, we used the expression data of CPXM1 in The Cancer Genome Atlas database to predict CPXM1-related signaling pathways through bioinformatics analysis.

Results

The expression level of CPXM1 in GC tissues was significantly correlated with tumor size ($p = 0.041$) and lymph node metastasis ($p = 0.014$). In addition, Kaplan–Meier analysis showed that the expression of CPXM1 in GC tissues was significantly associated with poor prognosis ($p = 0.011$). Multivariate analysis indicated that CPXM1 is a potential predictor of poor prognosis in GC patients ($p = 0.026$). The results of biosynthesis analysis demonstrated that the data set of CPXM1 high expression was mainly enriched in cancer-related signal pathways.

Conclusion

CPXM1 is an effective biomarker for the prognosis of GC patients and may play a key role in the occurrence and progression of GC.

Introduction

GC is one of the most common tumors of the digestive system and has been the fifth most common malignant cancer in the past decade. As the third leading cause of cancer deaths, the mortality rate of GC is increasing worldwide [1–2]. Although treatment methods (e.g., surgery, radiotherapy, chemotherapy) have improved, the prognosis of patients with advanced GC is still poor [3]. Therefore, it will be important to identify effective biomarkers to diagnose GC and predict prognosis.

The carboxypeptidase X, M14 family member (CPXM1) gene is located on chromosome 20p13 and is a member of the carboxypeptidase (CP) superfamily, which is a class of exopeptidases that specifically

degrades and releases free amino acids from the C-terminus of a peptide chain. Unlike most other members of the CP family, CPXM1 is inactive toward standard CP substrates, which could lack two residues related substrate binding such as Arg117 and Try248 in CPB [4]. Specifically, CPXM1 contains a discoidin domain (DSD), which consists of 157 amino acids and can bind the GVMGFO motif of collagen III. CPXM1 is a secreted protein predicted to contain four N-glycosylation sites, and its secretion is inhibited by the use of tunicamycin which is an inhibitor of N-acetylglucosamine phosphotransferase [5]. During osteoclastogenesis and adipogenesis, the expression level of CPXM1 has been shown to increase transiently, suggesting CPXM1 plays a key role in osteoclast and adipocyte differentiation [6–7].

At present, the biological function and molecular mechanism of CPXM1 in cancer have not been reported. Therefore, it is meaningful to study the relationship between CPXM1 and cancer. This study investigated the relationship between the clinicopathological features and prognosis of GC patients by immunohistochemistry (IHC) analysis, and analyzed the expression, prognosis, and related signaling pathways of CPXM1 in GC by bioinformatics analysis.

Materials And Methods

Public data extraction and processing

The gene expression quantification data and clinical data of 375 GC samples and 32 normal samples were downloaded from the GDC data portal (https://portal.gdc.cancer.gov/). We used Perl (https://www.perl.org/) scripts to decompress the downloaded compressed files in batches, which contain gene expression and clinical data of GC samples. Then, all sample IDs and RNA-seq data were integrated into a matrix file. Next, according to the Ensembl database (http://asia.ensembl.org/index.html), the Ensembl ID was converted to the gene symbol. Finally, we added the gene attribute (protein coding or lincRNA) after the gene symbol for subsequent operations. R (https://www.r-project.org/) language scripts and various packages were used to make the images and process the data. The expression difference of CPXM1 in normal gastric and GC tissues was verified in the Oncomine database (https://www.oncomine.org). The threshold was set to the following parameters: *p*-value of 0.001, fold change of 2, and gene rank of all. The correlation between CPXM1 expression and prognosis in GC patients was evaluated by Kaplan–Meier plotter (http://kmplot.com).

Patients and tissue samples

Informed consent was signed by all patients and their relatives, and the study was approved by the ethics committee of the First Affiliated Hospital, Yijishan Hospital of Wannan Medical College. All tissue samples containing 96 cases of GC tissues and 84 cases of paired normal tissues, which excluded patients with preoperative radiotherapy or chemotherapy, were processed anonymously in accordance with ethics and law.

IHC staining

The TMA was placed in an oven at 63°C for 1 h, and then placed in an automatic dyeing machine for dewaxing (LEICA). The TMA was soaked twice in xylene solution for 15 min and dehydrated in different concentrations of ethanol solution in sequence (100%, 7 min; 100%, 7 min; 90%, 7 min; 80%, 7 min; 70%, 7 min). The TMA was taken out and washed three times with pure water for 3 min, placed into boiling citric acid repair solution (82 ml 0.1 mol/L sodium citrate solution, 18 ml 0.1 mol/L citric acid solution, 900 ml pure water), heated in a pressure cooker for 5 min, and finally cooled to room temperature. The TMA was then placed into endogenous peroxidase blocking solution (38.4 ml anhydrous methanol, 12 ml 30% H_2O_2, 9.6 ml pure water) for 10 min, and then washed three times with phosphate-buffered saline (PBS) for 5 min. The TMA was covered with CPXM1 primary antibody (1:200; catalog no. bs-8341R, BIOSS, China) and placed at 4℃ overnight. The following day, the TMA was washed three times with phosphate-buffered saline (PBS) for 5 min and incubated with the secondary antibody (DAKO) at room temperature for 30 min followed by three washes with PBS for 5 min. Diluted DAB (DAKO) solution was added for 5 min and the TMA was washed with water for 15 min followed by the addition of hematoxylin for 2 min. The TMA was then immersed in 0.25% hydrochloric acid alcohol for 2 s and washed with water for 2 min. Finally, the TMA was placed into the automatic dyeing machine for dehydration and sealed with paraffin wax.

IHC evaluation

Two pathologists independently evaluated the immunohistochemical results of all samples in a blinded manner. When there were conflicting results, we invited a third pathologist to resolve the dispute. Cytoplasmic staining was positive, which was consistent with the description of primary antibody's instruction. We scored according to the staining intensity (negative = 0, weakly positive = 1, moderate positive = 2, strong positive = 3) and the percentage of stained cells (0–10% = 1, 11–50% = 2, 50–75% = 3, and 75–100% = 4). The results of the two scores were multiplied to obtain the immunohistochemical scores of all GC patients, and the GC patients were reasonably divided into a high expression group (score $\leq$ 3) and a low expression group (score > 3) by X-tile software.

Gene set enrichment analysis (GSEA)

GSEA was performed using GSEA v3.0 (https://www.gsea-msigdb.org) and JAVA 8 (https://www.java.com) to identify CPXM1 associated with gene sets. First, two files were prepared: (1) a .gct file containing CPXM1 expression data of 375 GC patients, and (2) a .cls file that divides the expression data of CPXM1 into high expression and low expression. Then, the number of permutations was set to 1000 to test CPXM1 correlations with the phenotypes using the c2.cp.kegg.v6.2 gene set database. Ultimately, with the normalized (NOM) *p*-value < 0.05 and false discovery rate (FDR) < 0.05, the gene sets with significant enrichment of CPXM1 high expression-related genes were considered the enrichment gene sets.

Gene Ontology (GO) and Kyoto Encyclopedia of Genes and Genomes (KEGG) analysis

To find the co-expressed genes of CPXM1, we first merged the same gene expression data in the processed matrix file and took the average. Secondly, the gene expression data of all the coding proteins in the matrix file was screened out, and the correlation was tested with the expression data of CPXM1 one by one.

Finally, we screened out co-expressed genes of CPXM1 using Pearson's correlation coefficient > 0.4 and *p*-value < 0.05 as thresholds. Then, we used R language scripts and R packages to perform GO and KEGG enrichment analyses. We considered the co-expressed genes of CPXM1 significantly enriched in the GO term and the KEGG pathway at *p*-value < 0.05 and FDR *q*-value < 0.05.

Statistical analysis

SPSS 23.0, GraphPad prism 8.0.2, and R 4.0.2 were used for statistical analysis. The Chi square test and Fisher's exact test were performed to detect the correlation between CPXM1 expression levels and clinicopathological features in the 90 GC patients. The Kaplan–Meier survival curve and log-rank test were used to compare the survival rate between the CPXM1 high expression and low expression groups. We performed univariate Cox-regression analysis of all clinicopathological parameters, and then integrated these parameters into multivariate Cox-regression analysis to determine independent predictors of survival in GC patients. *p*-values < 0.05 were considered statistically significant.

Results

Relationship between CPXM1 mRNA expression and clinicopathological features, and survival of GC patients in public databases

We first verified that the expression level of CPXM1 mRNA was significantly increased in GC tissues in the Oncomine database ($p < 0.001$) **(Figure 1A–C)**. Secondly, we screened the CPXM1 expression data of 375 GC patients and 32 normal patients downloaded from The Cancer Genome Atlas (TCGA) database, and confirmed that the expression level of CPXM1 mRNA in GC tissues was 4.87 times higher than that in normal tissues ($p < 0.001$) **(Figure 1D)**. At the same time, comparison of paired GC tumors and normal tissues also showed that the expression level of CPXM1 mRNA was significantly upregulated ($p < 0.001$) **(Figure 1E)**. Then, we analyzed the relationship between the expression level of CPXM1 mRNA and clinicopathological features of these patients, and found that the tumor invasion grade was significantly correlated with CPXM1 expression ($p < 0.001$) **(Figure 1F)**. Finally, we analyzed the relationship between the expression level of CPXM1 and the survival of GC patients through the Kaplan–Meier plotter database. The results showed that the prognosis of GC patients with high expression of CPXM1 was significantly poor ($p < 0.001$) **(Figure 1G)**. These data indicate that CPXM1 plays an important role in the occurrence and progression of GC.

Relationship between CPXM1 expression of GC and normal tissues and clinicopathological features and survival in a TMA

To verify CPXM1 expression at the protein level, a TMA containing 96 GC tissues and 84 normal tissues was subjected to immunohistochemistry (**Figure 2**). These samples had complete clinicopathological features and survival follow-up information. In this study, the expression of CPXM1 was high in 46 cases of GC tissues and 34 cases of normal tissues. However, there was no significant difference in the expression of CPXM1 between GC and normal tissues ($p = 0.824$, **Table 1**). Subsequently, we analyzed the relationship between the expression of CPXM1 and clinicopathological features in GC and normal tissues, separately

(**Table 2**). The expression level of CPXM1 in GC tissues was significantly correlated with tumor size ($p = 0.041$) and lymph node metastasis ($p = 0.014$), but not with gender, age, pathological grade, tumor invasion, distant metastasis, and AJCC stage (all $p > 0.05$). In addition, the expression level of CPXM1 in normal tissues was not statistically significant with all clinicopathological features (all $p > 0.05$).

According to the Kaplan–Meier survival curve analysis, we found that survival in patients with high expression of CPXM1 in GC tissues was significantly correlated with prognosis ($p = 0.011$, **Figure 3A**). However, CPXM1 high expression in normal tissues was not significantly correlated with the prognosis of GC patients ($p = 0.317$, **Figure 3B**). Univariate analysis showed that tumor size (hazard ratio [HR] = 2.054, 95% confidence interval [CI] [1.216–3.468], $p = 0.007$), pathological grade (HR = 3.051, 95% CI [1.217–7.651], $p = 0.017$), tumor invasion (HR = 4.084, 95% CI [1.276–13.078], $p = 0.018$), lymph node metastasis (HR = 3.569, 95% CI [1.914–6.655], $p < 0.001$), distant metastasis (HR = 7.255, 95% CI [1.706–30.809], $p = 0.007$), ACJJ stage (HR = 2.809, 95% CI [1.646–4.792], $p < 0.001$), and CPXM1 expression (HR = 2.001, 95% CI [1.165–3.435], $p = 0.012$) were associated with overall survival. Multivariate analysis showed that pathological grade (HR = 2.581, 95% CI [1.011–6.595], $p = 0.047$) and CPXM1 expression (HR = 1.880, 95% CI [1.078–3.277], $p = 0.026$) were independent prognostic factors (**Table 3**). These results suggest that CPXM1 could be a potential independent prognostic factor in GC patients.

GSEA analysis of CPXM1-related signaling pathways

We performed GSEA analysis on both the CPXM1 high expression and low expression datasets in TCGA to identify various pathways that could be activated in GC. Using NOM p-value < 0.05 and FDR q-value < 0.05 as the threshold, we listed the first 20 pathways related to the CPXM1 high expression data set; most of these pathways were related to cancer phenotypes (**Table 4**). Pathways associated with focal adhesion, cell adhesion molecules (CAMs), extracellular matrix (ECM) receptor interaction, cytokine-cytokine receptor interaction, leukocyte transendothelial migration, dilated cardiomyopathy, axon guidance, melanoma, and Hedgehog signaling pathway were enriched in the CPXM1 high expression data set (**Figure 4**).

GO and KEGG analyses of CPXM1 co-expressed genes

To further elucidate the molecular mechanism of CPXM1 in GC, we screened CPXM1 co-expressed genes from the TCGA database and visualized their correlation (**Figure 5A**). We then analyzed the CPXM1 co-expressed gene expression correlation by GO and KEGG analyses. GO analysis showed that the CPXM1 co-expressed genes were mainly enriched in ECM structural constituent, cell adhesion molecule binding, glycosaminoglycan binding, and integrin binding (**Figure 5B**). In addition, KEGG analysis showed that CPXM1 co-expressed genes were mainly enriched in signaling pathways related to focal adhesion, ECM-reporter interaction, proteoglycans in cancer, and osteoclast differentiation, and participated in some classic cancer-related signaling pathways, such as PI3K-Akt and Rap1 signaling (**Figure 5C**). Chord plot displays of the relationship between CPXM1 co-expressed genes and KEGG pathways are shown in **Figure 5D**. The CPXM1 co-expressed gene profiles are displayed in each KEGG pathway by hierarchical clustering (**Figure 5E**). Therefore, based on our bioinformatics analysis we conclude that CPXM1 could activate a series of cancer-related signaling pathways through ECM interactions, which may lead to malignant

phenotypes such as cancer adhesion and metastasis. These results are consistent with the CPXM1-related clinicopathological parameters described above.

Discussion

GC is one of the most common malignant tumors worldwide. Although the cure rate of early GC is very high, the 5-year survival rate is only 3.9% once metastasis occurs [8]. The molecular mechanisms of GC metastasis are complex, and so it is particularly important to identify independent prognostic factors for GC. We hypothesized that CPXM1 may play a key role in the development of GC through multiple databases, and the molecular mechanisms of CPXM1 in cancer have not been reported at present. Therefore, we proposed for the first time that the expression of CPXM1 in GC was related to the clinicopathological characteristics and survival of GC patients in this study, and predicted CPXM1 related signaling pathways through bioinformatics analysis, laying the foundation for subsequent experiments.

CPXM1 is a member of the CPE family, and a special member of the CP family along with CPXM2 and AEBP1 [5]. Overexpression of CPXM2 is closely related to the prognosis of GC patients, and may promote the proliferation and invasion of GC through the epithelial–mesenchymal transition [9]. AEBP1 could be a potential prognostic factor for GC, which can activate NF-κB signaling and lead to a series of malignant phenotypes of GC [10]. First, compared with other members, CPXM1, CPXM2, AEBP1 are highly homologous. Second, they seem to lack CP activity, which may be caused by the deletion of CP-related active sites or the substitution of other residues. Finally, they are unique in that their signal peptides are connected via a DSD [11].

The DSD is composed of approximately 150 amino acids. It is widely distributed in secretory proteins, intracellular proteins, and transmembrane proteins, and participates in a variety of biological functions. The DSD structure of AEBP1 may interact with collagen I to regulate the spreading and proliferation of fibroblasts and myofibroblasts [12]. In addition, special sites in the DSD of DDR1 and DDR2 can bind different collagen proteins, and activate a series of downstream signaling pathways to promote the malignant phenotypes of various cancer cells [13]. Kim et al. found that the homology of CPXM1 DSD with CPXM2 and AEBP1 was 58.9% and 53.2%, respectively, and that of DDR1 and DDR2 was 34.7% and 34.2%. CPXM1, like DDR1, DDR2, and AEBP1, could bind the GVMGFO motif of collagen III [5]. Early studies found that CPXM1 is a secretory protein associated with N-glycosylation. Four glycosylation sites were predicted, located at N57, N210, N318, and N472. N-glycosylation is closely related to the secretion of CPXM1. When tunicamycin was used to inhibit the formation of N-glycosylation, it was showed that the amount of CPXM1 secreted into the extracellular medium was significantly reduced [4–5].

Our immunohistochemical results showed that there was no difference in the expression of CPXM1 between GC and normal tissues. This may be due to the increased secretion of CPXM1 caused by glycosylation in gastric cancer tissue, and our preliminary experiments results show that compared with normal gastric mucosa tissue, the glycosylation of CPXM1 in gastric cancer tissue is significantly increased (not shown). However, the expression level of CPXM1 in GC tissues was closely related to some clinicopathological features and the prognosis of GC patients. Through univariate and multivariate

analyses, CPXM1 was determined to be an independent prognostic factor for GC patients. The results of GSEA showed that the high expression of CPXM1 enriched for signaling pathways related to focal adhesion, cell adhesion molecules, and ECM-receptor interaction. To further verify the results, we performed GO and KEGG analyses and found that the co-expression genes of CPXM1 were enriched in cell adhesion-related signaling pathways, such as focal adhesion, PI3K-Akt signaling pathway, integrin binding, and cell adhesion molecular binding. Cell matrix adhesion plays an important role in cell movement, cell proliferation, cell differentiation, and cell survival. Focal adhesion refers to the special structure of actin filaments anchored on the transmembrane receptor of the integrin family through the multimolecular complex connecting plaque protein [14]. These structures can activate downstream signaling pathways, leading to reorganization of the actin cytoskeleton, which is a key prerequisite for changing cell shape, movement, and gene expression [15–16]. The relationship between CPXM1 and the cell adhesion pathway needs to be further studied.

There are three important limitations in our research. First, we used a relatively small number of TMA samples and used retrospective studies to analyze GC tissues, which may lead to potential bias. Second, we only collected the overall survival time, so we could not analyze the relationship between CPXM1 expression and disease-free survival and relapse-free survival. Finally, the molecular mechanism of CPXM1 in GC is not clear due to a lack of experiments.

In conclusion, the overexpression of CPXM1 may indicate a poor prognosis of GC. In addition, our bioinformatics results showed that CPXM1 may regulate the cell adhesion-related signaling pathway of GC. However, further experiments are needed to study the precise molecular mechanism of CPXM1 in GC.

Abbreviations

CPXM1 carboxypeptidase X, M14 family member

GC gastric cancer

CP carboxypeptidase

DSD discoidin domain

IHC immunohistochemistry

TMA the tissue microarray

PBS phosphate-buffered saline

GO gene ontology

KEGG kyoto encyclopedia of genes and genomes

CAMs cell adhesion molecules

ECM extracellular matrix

Declarations

Acknowledgments

We thank the teachers of the Central Laboratory, Yijishan Hospital of Wannan Medical College for providing constructive suggestions for this study. DJ is grateful for the silent support of HYM.

Funding

The authors declare that there are no sources of funding to be acknowledged.

Availability of data and materials

All datasets were submitted in the supplementary materials (All download links are in the “Materials and Methods” section).

Authors' Contribution

DJ designed the study and wrote the manuscript. ZMX, YWW, YCS, and LQY extracted the data from various public databases. DJ processed the data through R and Perl software. WJG resolved any disputes, provided critical evaluation and supervised the study. All authors contributed to this article and agreed to publish the final manuscript.

Ethics approval and consent to participate

The study was approved by the ethics committee of the First Affiliated Hospital, Yijishan Hospital of Wannan Medical College, and written informed consent was received from the patients.

Consent for publication

Not applicable.

Competing Interests

The authors declare that there are no competing interests associated with the manuscript.

References

[1] J. Ferlay, H.R. Shin, F. Bray, D. Forman, C. Mathers, D.M. Parkin, Estimates of worldwide burden of cancer in 2008: GLOBOCAN 2008, Int. J. Cancer, 127 (2010) 2893–2917. https://doi.org/10.1002/ijc.25516

[2] F. Bray, J. Ferlay, I. Soerjomataram, R.L. Siegel, L.A. Torre, A. Jemal, Global cancer statistics 2018: GLOBOCAN estimates of incidence and mortality worldwide for 36 cancers in 185 countries, CA. Cancer J. Clin. 68 (2018) 394–424. https://doi.org/10.3322/caac.21492

[3] Y. Isobe, A. Nashimoto, K. Akazawa, I. Oda, K. Hayashi, I. Miyashiro, H. Katai, S. Tsujitani, Y. Kodera, Y. Seto, M. Kaminishi, Gastric cancer treatment in Japan: 2008 annual report of the JGCA nationwide registry, Gastric Cancer, 14 (2011) 301–316. https://doi.org/10.1007/s10120-011-0085-6

[4] Y. Lei, X. Xin, D. Morgan, J.E. Pintar, L.D. Fricker, Identification of mouse CPX-1, a novel member of the metallocarboxypeptidase gene family with highest similarity to CPX-2, DNA Cell Biol. 18 (1999) 175–185. https://doi.org/10.1089/104454999315565

[5] Y.H. Kim, H.M. O'Neill, J.P. Whitehead, Carboxypeptidase X-1 (CPX-1) is a secreted collagen-binding glycoprotein, Biochem. Biophys. Res. Commun. 468 (2015) 894–899. https://doi.org/10.1016/j.bbrc.2015.11.053

[6] E.J. Chang, H.B. Kwak, H. Kim, J.C. Park, Z.H. Lee, H.H. Kim, Elucidation of CPX-1 involvement in RANKL-induced osteoclastogenesis by a proteomics approach, FEBS Lett. 564 (2004) 166–70. https://doi.org/10.1016/S0014-5793(04)00338-2

[7] Y.H. Kim, J.L. Barclay, J. He, X. Luo, H.M. O'Neill, S. Keshvari, J.A. Webster, C. Ng, L.J. Hutley, J.B. Prins, J.P. Whitehead, Identification of carboxypeptidase X (CPX)-1 as a positive regulator of adipogenesis, FASEB J. 30 (2016) 2528–2540. https://doi.org/10.1096/fj.201500107R

[8] Y. Zhang, Y. Lin, J. Duan, K. Xu, M. Mao, X. Wang, A population-based analysis of distant metastasis in stage iv gastric cancer, Med. Sci. Monit. 26 (2020) 1–18. https://doi.org/10.12659/MSM.923867

[9] J. Liu, L. Jiang, J. Liu, T. He, Y. Cui, F. Qian, P. Yu, AEBP1 promotes epithelial-mesenchymal transition of gastric cancer cells by activating the NF-KB pathway and predicts poor outcome of the patients, Sci. Rep. 8 (2018) 1–13. https://doi.org/10.1038/s41598-018-29878-6

[10] G. Niu, Y. Yang, J. Ren, T. Song, Z. Hu, L. Chen, R. Hong, J. Xia, C. Ke, X. Wang, Overexpression of CPXM2 predicts an unfavorable prognosis and promotes the proliferation and migration of gastric cancer, Oncol. Rep. 42 (2019) 1283–1294. https://doi.org/10.3892/or.2019.7254

[11] S.E. Reznik , L.D. Fricker, Carboxypeptidases from A to Z: Implications in embryonic development and Wnt binding, Cell. Mol. Life Sci. 58 (2001) 1790–1804. https://doi.org/10.1007/PL00000819

[12] S.L. Schissel, S.E. Dunsmore, X. Liu, R.W. Shine, M.A. Perrella, M.D. Layne, Aortic carboxypeptidase-like protein is expressed in fibrotic human lung and its absence protects against bleomycin-induced lung fibrosis, Am. J. Pathol. 174 (2009) 818–828. https://doi.org/10.2353/ajpath.2009.080856

[13] R.R. Valiathan, M. Marco, B. Leitinger, C.G. Kleer, R. Fridman, Discoidin domain receptor tyrosine kinases: New players in cancer progression, Cancer Metastasis Rev. 31 (2012) 295–321. https://doi.org/10.1007/s10555-012-9346-z

[14] S.H. Lo , L.B. Chen, Focal adhesion as a signal transduction organelle, Cancer Metastasis Rev. 13 (1994) 9–24. https://doi.org/10.1007/BF00690415

[15] F.G. Giancotti, G. Tarone, Positional control of cell fate through joint integrin/receptor protein kinase signaling, Annu. Rev. Cell Dev. Biol. 19 (2003) 173–206. https://doi.org/10.1146/annurev.cellbio.19.031103.133334

[16] R.O. Hynes, Integrins: bidirectional, allosteric signaling machines, Cell. 110 (2002) 673–687. https://doi.org/10.1016/s0092-8674(02)00971-6

Tables

Table 1. Relationship between GC tissues and normal tissues.

		Cancer tissue		Correlation	*P*-value
		L	H		
Normal tissue	L	18	24	0.049	0.824
	H	16	26		
L: CPXM1 low expression; H: CPXM1 high expression					

Table 2. Association between CPXM1 expression in GC tissues and paired normal tissues and clinicopathological features of GC patients.

Variables	Cancer tissue				Normal tissue			
	L	H	c^2	*P*-value	L	H	c^2	*P*-value
Age (years)			0.909	0.403			0.064	0.822
< 60	20	17			12	19		
³ 60	26	33			22	31		
Gender			0.004	1.000			1.265	0.327
Male	31	34			22	38		
Female	15	16			12	12		
Tumor size			4.455	**0.041***			0.191	0.823
< 6 cm	31	23			20	27		
³ 6 cm	15	27			14	23		
Pathological grade			0.033	1.000			2.838	0.087
£ 2	8	8			3	13		
> 2	38	42			31	37		
Tumor invasion			0.035	0.998			4.368	0.224
T1	1	1			0	2		
T2	5	6			5	6		
T3	24	26			21	22		
T4	16	17			8	20		
Lymph node metastasis			10.664	**0.014***			3.640	0.303
N0	12	8			8	10		
N1	16	9			6	12		
N2	10	9			13	11		
N3	8	24			7	17		
Distant metastasis			0.430	0.496			0.000	1.000
M0	46	48			34	49		
M1	0	2			0	1		
ACJJ stage			3.503	0.320			1.080	0.782
Stage I	5	3			4	4		

Stage II	15	12	9	15
Stage III	26	33	21	30
Stage IV	0	2	0	1

L: CPXM1 low expression; H: CPXM1 high expression; *P value < 0.05 was considered statistically significant.

Table 3. Univariate and multivariate analyses of overall survival of GC patients.

Variables	Univariate analysis			Multivariate analysis		
	HR	95% CI	P-value	HR	95% CI	P-value
Age (years)	1.332	0.767- 2.311	0.309			
Gender	0.899	0.518- 1.559	0.703			
Tumor size	2.054	1.216- 3.468	**0.007***			
Pathological grade	3.051	1.217- 7.651	**0.017***	2.581	1.011- 6.595	**0.047***
Tumor invasion	4.084	1.276- 13.078	**0.018***			
Lymph node metastasis	3.569	1.914- 6.655	**< 0.001***			
Distant metastasis	7.255	1.706- 30.809	**0.007***			
ACJJ stage	2.809	1.646- 4.792	**< 0.001***			
CPXM1 expression	2.001	1.165- 3.435	**0.012***	1.880	1.078- 3.277	**0.026***

**P* value < 0.05 was considered significant.

Table 4. CPXM1 high expression dataset significantly enriched on GSEA terms.

	GSEA team	Size	ES	NES	NOM p-val	FDR q-val
1	KEGG_FOCAL_ADHESION	197	0.76	2.56	0	0
2	KEGG_CELL_ADHESION_MOLECULES_CAMS	128	0.77	2.41	0	0
3	KEGG_ECM_RECEPTOR_INTERACTION	84	0.83	2.41	0	0
4	KEGG_CYTOKINE_CYTOKINE_RECEPTOR_INTERACTION	257	0.66	2.39	0	0
5	KEGG_LEUKOCYTE_TRANSENDOTHELIAL_MIGRATION	115	0.7	2.37	0	0
6	KEGG_DILATED_CARDIOMYOPATHY	90	0.69	2.31	0	0
7	KEGG_AXON_GUIDANCE	127	0.65	2.3	0	0
8	KEGG_MELANOMA	71	0.64	2.29	0	0
9	KEGG_HEDGEHOG_SIGNALING_PATHWAY	56	0.69	2.29	0	0
10	KEGG_HYPERTROPHIC_CARDIOMYOPATHY_HCM	83	0.67	2.28	0	0
11	KEGG_CHEMOKINE_SIGNALING_PATHWAY	184	0.67	2.28	0	0
12	KEGG_REGULATION_OF_ACTIN_CYTOSKELETON	211	0.59	2.27	0	0
13	KEGG_PATHWAYS_IN_CANCER	321	0.6	2.27	0	0
14	KEGG_HEMATOPOIETIC_CELL_LINEAGE	85	0.74	2.26	0	0
15	KEGG_LEISHMANIA_INFECTION	70	0.76	2.19	0	0
16	KEGG_GAP_JUNCTION	88	0.6	2.18	0	0
17	KEGG_TOLL_LIKE_RECEPTOR_SIGNALING_PATHWAY	101	0.62	2.18	0	0
18	KEGG_MAPK_SIGNALING_PATHWAY	265	0.56	2.18	0	0
19	KEGG_RENAL_CELL_CARCINOMA	66	0.65	2.16	0	0.001
20	KEGG_BASAL_CELL_CARCINOMA	55	0.68	2.16	0	0.001

Figures

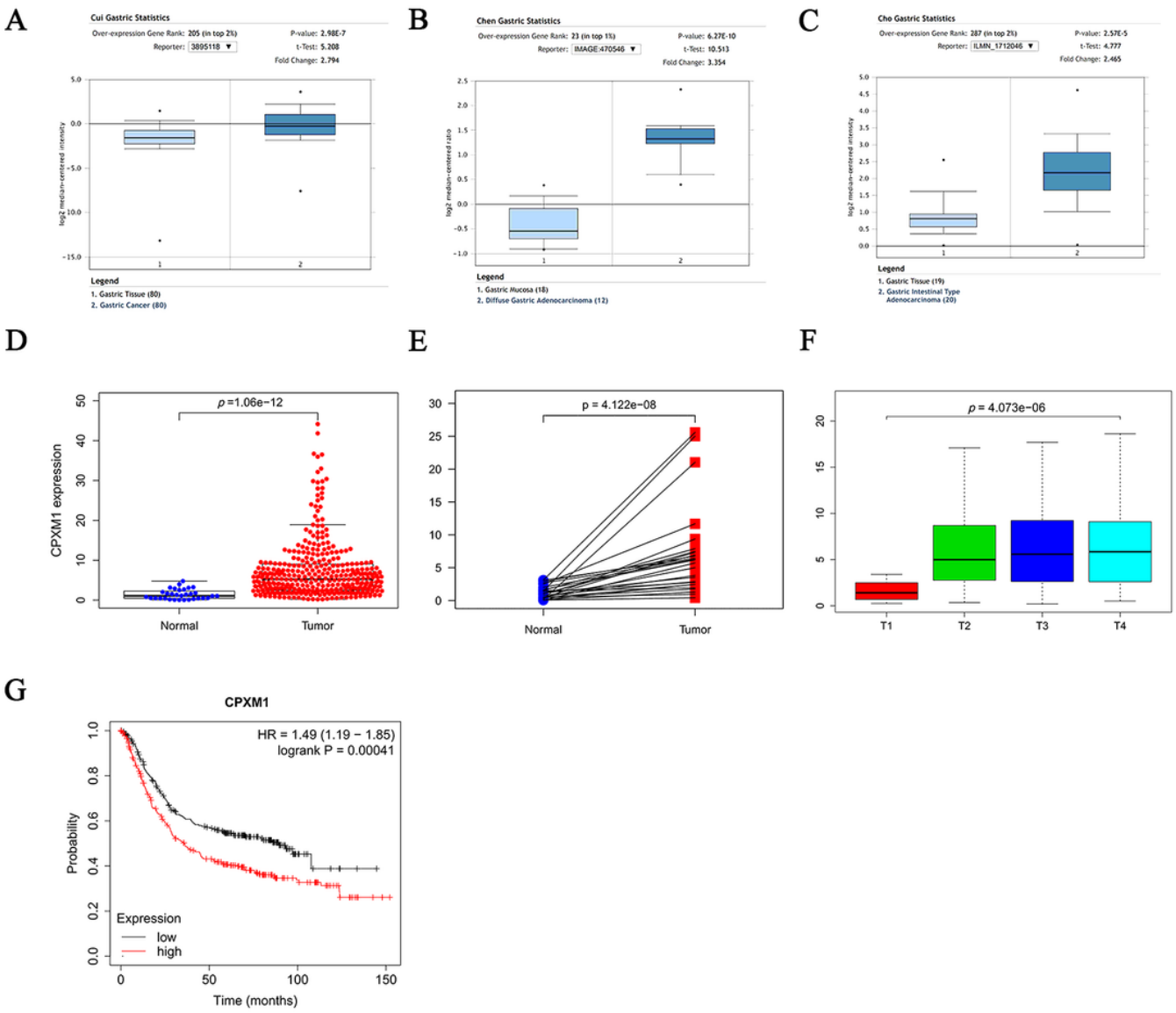

Figure 1

CPXM1 is upregulated in gastric cancer tissues and correlates with poor survival. (A–C) The Cui, Chen, and Cho gastric analyses in the Oncomine database are presented, illustrating the overexpression of CPXM1 in GC tissues. (D) According to TCGA-STAD data, a dot plot representing the expression level of CPXM1 in GC tissues (red dots, n = 375) and normal tissues (blue dots, n = 32) is shown. (E) Expression of CPXM1 in GC tissues (red dots, n = 32) and paired normal tissues (blue dots, n = 32). (F) Association between CPXM1 expression and T classification. (G) Impact of CPXM1 expression on overall survival in GC patients. Data were retrieved from the Kaplan–Meier plotter database.

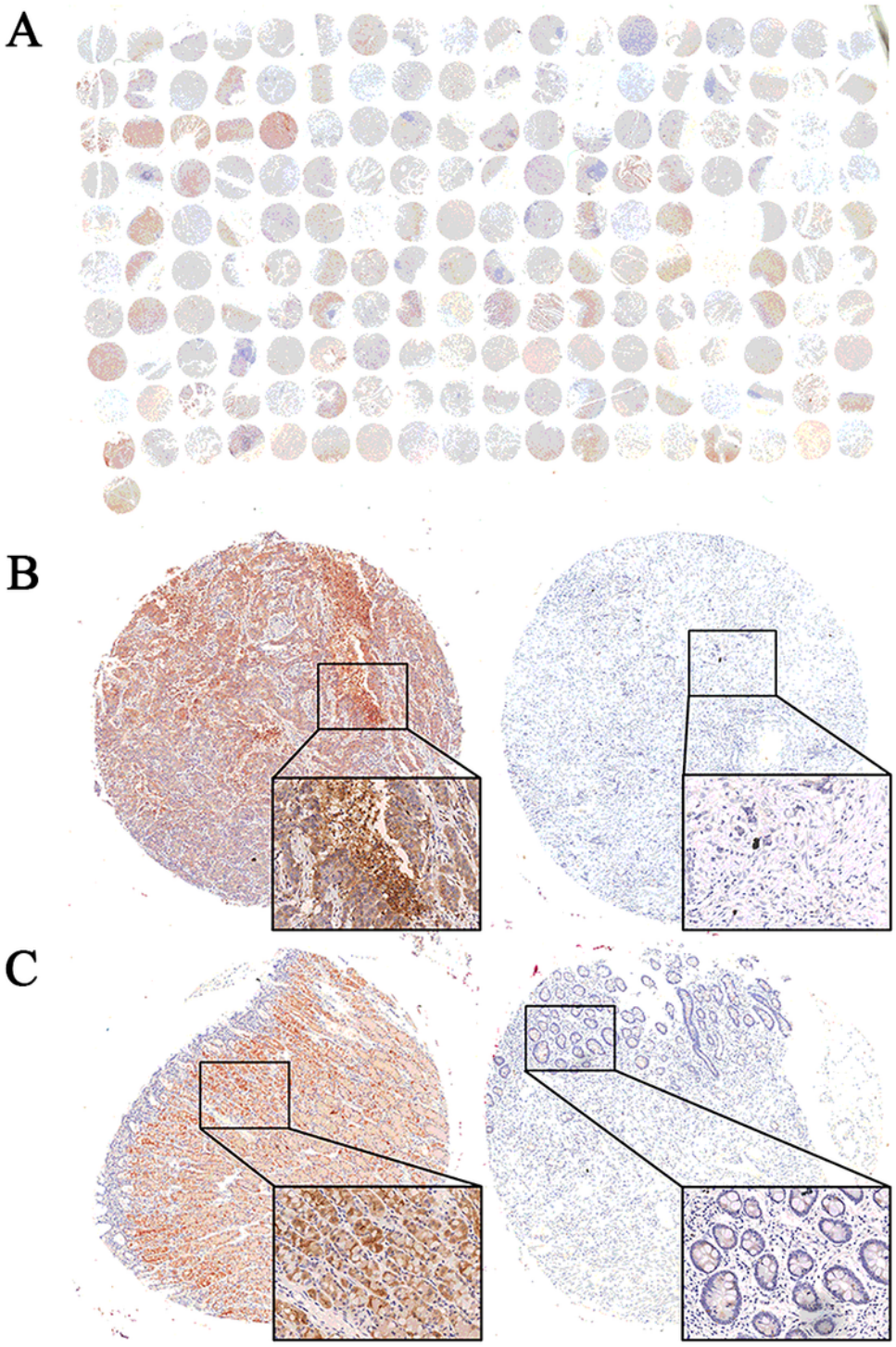

Figure 2

TMA and IHC staining of CPXM1 in GC tissues. (A) TMA containing 96 cases of GC tissues and 84 cases of paired normal tissues; 1× magnification. (B) High CPXM1 expression (left) and low CPXM1 expression (right) in GC tissue staining; 100× magnification in the bottom right corner. (C) High CPXM1 expression (left) and low CPXM1 expression (right) in normal tissue staining; 100× magnification in the bottom right corner.

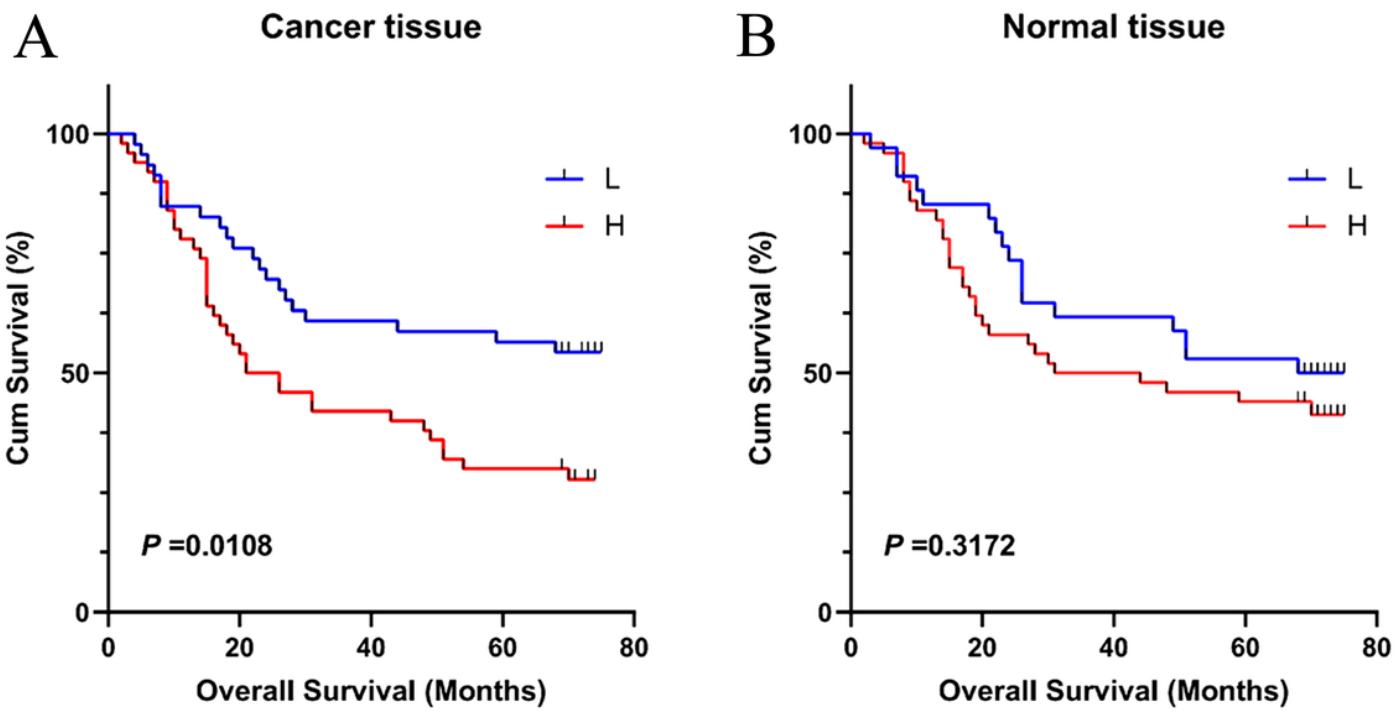

Figure 3

Kaplan–Meier curves illustrate that the overall survival time of patients with CPXM1 high expression GC tissues (left) and normal tissues (right) correlated with prognosis.

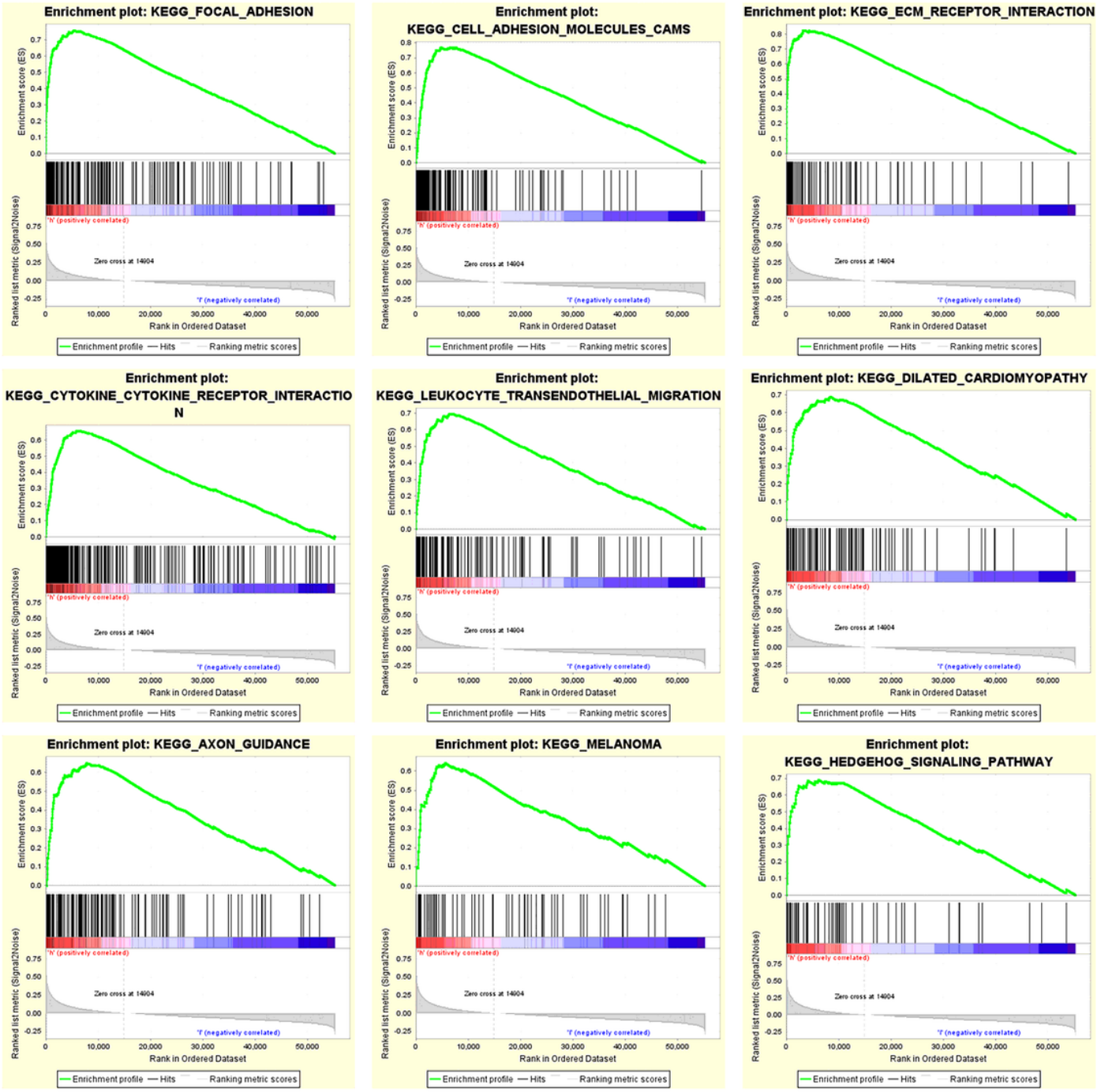

Figure 4

Enrichment plots of CPXM1 high expression data set from GSEA analysis. The CPXM1 high expression data set was enriched in focal adhesion, cell adhesion molecules, ECM-receptor interaction, cytokine-cytokine receptor interaction, leukocyte transendothelial migration, dilated cardiomyopathy, axon guidance, melanoma, and Hedgehog signaling pathway.

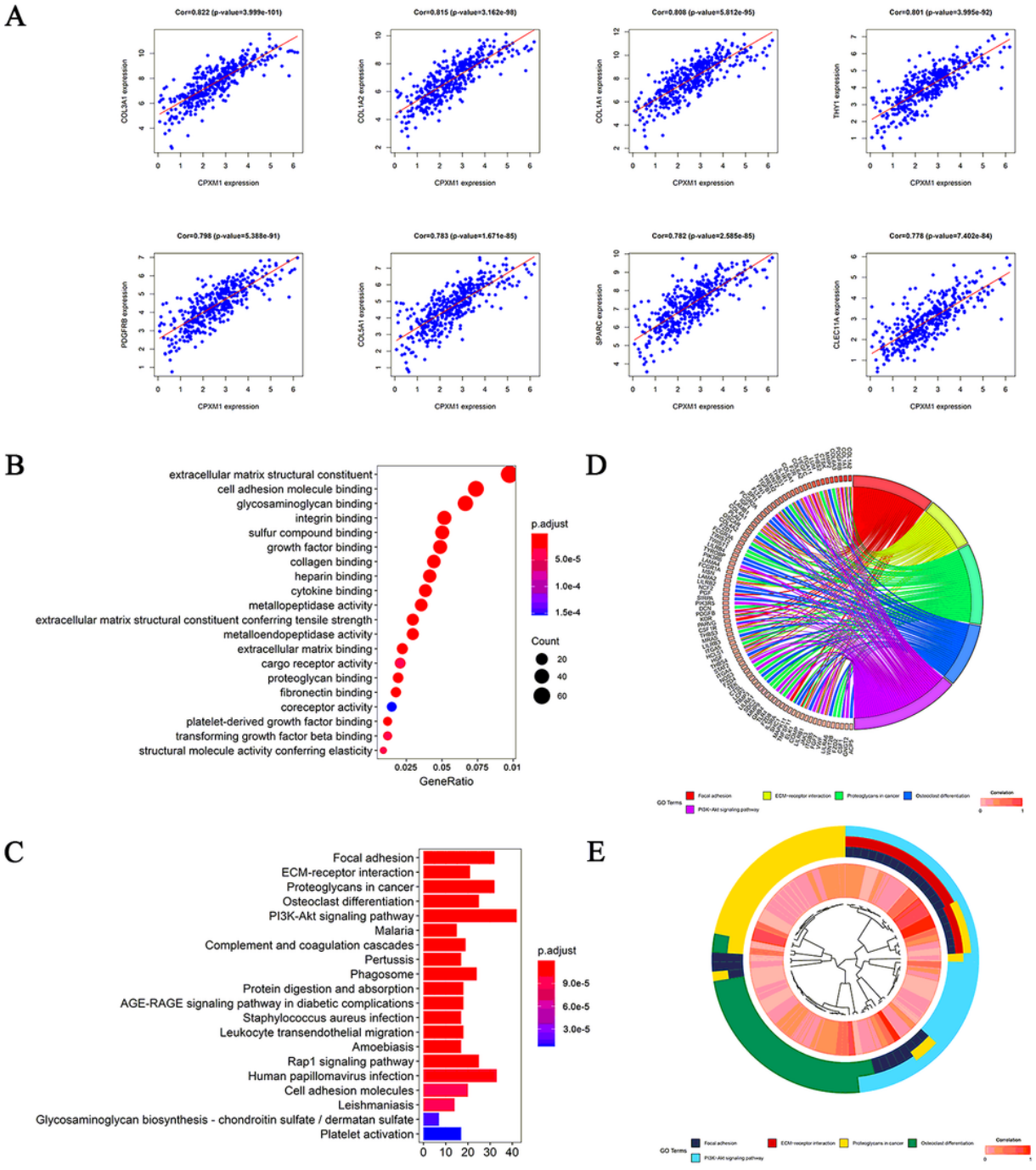

Figure 5

GO and KEGG analyses of CPXM1 co-expressed genes in TCGA database. (A) The most relevant co-expressed genes of CPXM1, including COL3A1, COL1A2, COL1A1, THY1, PDGFRB, COL5A1, SPARC, and CLEC11A. (B) CPXM1 co-expressed genes in TCGA were enriched in biological processes related to extracellular matrix and cell adhesion. (C) CPXM1 co-expressed genes in TCGA were enriched in KEGG pathways related to cell adhesion and migration. (D) Hierarchical clustering of the CPXM1 co-expressed

gene profiles in each KEGG pathway. (E) Chord plot displays of the relationship between the CPXM1 co-expressed genes and KEGG pathways.

Supplementary Files

This is a list of supplementary files associated with this preprint. Click to download.

- Supfiles1.doc
- Supfiles2.xls
- Supfiles3.xls
- Supfiles4.docx